Available online at www.sciencedirect.com
ScienceDirect
Biochimica et Biophysica Acta 1768 (2007) 1268 – 1276
Biochimica et Biophysica Acta
BBA
www.elsevier.com/locate/bbamem

Roughness of the plasma membrane as an independent morphological parameter to study RBCs: A quantitative atomic force microscopy investigation

M. Girasole [a,*], G. Pompeo [a], A. Cricenti [a], A. Congiu-Castellano [b], F. Andreola [c], A. Serafino [c], B.H. Frazer [d], G. Boumis [e], G. Amiconi [e]

[a] *Istituto di Struttura della Materia–CNR, Via fosso del Cavaliere 100, 00133 Rome, Italy*
[b] *Dipartimento di Fisica–Università "La Sapienza", P.le Aldo Moro 5, 00185 Rome, Italy*
[c] *Istituto di Neurobiologia e Medicina Molecolare–CNR, Via fosso del Cavaliere 100, 00133 Rome, Italy*
[d] *Department of Physics University of Wisconsin–Madison and Synchrotron Radiation Center, Stoughton, WI 53589, USA*
[e] *Dipartimento di Scienze Biochimiche "A. Rossi-Fanelli"-Università "La Sapienza", P.le Aldo Moro 5, 00185 Rome, Italy*

Received 10 November 2006; received in revised form 8 January 2007; accepted 8 January 2007
Available online 26 January 2007

Abstract

A novel approach to the study of RBCs based on the collection of three-dimensional high-resolution AFM images and on the measure of the surface roughness of their plasma membrane is presented. The dependence of the roughness from several parameters of the imaging was investigated and a general rule for a trustful analysis and comparison has been suggested. The roughness of RBCs is a morphology-related parameter which has been shown to be characteristic of the single cells composing a sample, but independent of the overall geometric shape (discocyte or spherocyte) of the erythrocytes, thus providing extra-information with respect to a conventional morphology study. The use of the average roughness value as a label of a whole sample was tested on different kinds of samples. Analyzed data revealed that the quantitative roughness value does not change after treatment of RBCs with various commonly used fixation and staining methods while a drastic decrease occurs when studying cells with membrane–skeletal alteration both naturally occurring or artificially induced by chemical treatments. The present method provides a quantitative and powerful tool for a novel approach to the study of erythrocytes structure through an ultrastructural morphological analysis with the potential to give information, in a non-invasive way, on the RBCs function.

Keywords: Surface roughness; Atomic force microscopy; Membrane–skeleton structure

1. Introduction

Surface roughness is an important parameter for many applications which require characterization and/or a comparison of surfaces. The use of such a parameter has received a new impulse from the application of Scanning Probe Microscopy (SPM) techniques to many classes of studies [1,2]. In particular, atomic force microscopy (AFM) has emerged also in ultra-structural biology as a broadly used tool capable to provide a quantitative description of morphological details of rugged cell exterior or biomolecular assemblies under physiological and non-physiological conditions (e.g., dried or chemically fixed samples). Furthermore, all the quantitative values are obtained with a lateral resolution approaching few nanometers and a vertical sensitivity of the order of 1 Å.

In many applications, after acquiring an AFM image, the comparison of the distinctive features at the nanometer scale seen on the surface of two or more samples (i.e., their morphology), can be best described by statistical analysis rather than comparison of tiny structures strictly related to the local sample arrangement: in this framework roughness can be a useful tool. A variety of mathematical approaches can be applied to such a calculation, the most common consisting of the analysis of the surface data generated by an AFM in terms of the distribution of its heights. The roughness value of the

* Corresponding author.
E-mail address: marco.girasole@ism.cnr.it (M. Girasole).

0005-2736/$ - see front matter © 2007 Elsevier B.V. All rights reserved.
doi:10.1016/j.bbamem.2007.01.014

surface can be described in terms of the measure of the root–mean–square value of the height distribution. In other words:

$$R_{\mathrm{rms}} = \sqrt{\sum_{i=1}^{N} \frac{(z_i - z_{\mathrm{m}})^2}{(N-1)}} \quad (1.1)$$

where N is the total number of data points; z_i is the height of ith point and z_{m} is the mean height. It is worth noting that the surface roughness is, by definition, a morphology-related parameter.

Most studies make use of the R_{rms} since such a quantitative definition has the advantage of being a simple mathematical approach and it conserves the intuitive concept of a rugged surface [3,4]. Additionally, the R_{rms} is straightforward to be measured experimentally as the heights of the surface are the very points of an AFM image. The major limitation of the present R_{rms} definition is that it intrinsically contains a certain degree of degeneracy and lack of information about spatial coherence and, indeed, alternative methods to evaluate the surface texture have been suggested [5]. Some of these other methods, based on the computation of the variance correlation function, have been demonstrated to be capable of giving additional information by studying the scale-dependent or fractal behaviour of the sample surface at the price, however, of a substantially more complex mathematical framework.

Whatever the chosen definition of roughness be, such a parameter has been widely used in the past to compare surfaces of interest for surface science [6], biomaterials [7], organic and inorganic chemistry [8], while a lesser number of application involving living or fixed/stained cells have been attempted. This is mostly due to severe technical complications which make the comparison of cells surfaces not straightforward: for instance the complexity of biological samples and their intrinsic variability (i.e., the structural differences among single elements in a given class of cells).

One of the purposes of this study is to claim that, under suitable and well-defined conditions, the surface roughness can be precious in the quantitative study of the morphology of a biological membrane with interesting applications even in the study of the cell structure and function.

The size and shape of human red blood cells (RBCs) are important indicators of well being [9]; for this reason and for their relatively simple structure and ease of isolation, RBCs have been extensively studied over the years. It is generally believed that the plasma membrane is responsible for maintaining the shape of RBCs [10] and for permitting extensive, passive deformations that allow them to resist, without fragmentation, to repeated passages through narrow capillaries (the diameter of which being less than one half that of RBCs). As proposed by the bilayer couple hypothesis [11], the membrane is a composite structure in which the lipid bilayer is anchored through tethering sites (transmembrane proteins) to the membrane–skeleton, an underlying network of proteins localized in the cytoplasm of the cell. The typical biconcave shape of RBCs results from a variety of interactions between the cell and its environment and can be altered both in vitro (by several factors, including direct intercalation of phospholipids [12] or drugs [13] into the membrane), and in vivo (because of hereditary defects [14] or environmental-induced modifications [15] of the cell skeleton) and, indeed, even in blood stains from healthy donors a certain number of unusually shaped RBCs are present [16].

In studying these classes of morphological problems the use of an intrinsically three-dimensional, high-resolution, non-destructive surface characterizing technique such as AFM is very appropriate [17]. And, indeed, it has been used to image the RBCs' overall shape and their local surface under normal and pathological conditions [18–22] and to analyze in quantitative terms problems related to the membrane–skeleton elements that can be observed as isolated components [23,24] or as part of membrane patches [25,26].

In the present paper we used AFM technique to evaluate the surface roughness of RBCs treated in different ways. A set of optimal experimental conditions have been chosen in order to obtain an unambiguous interpretation of experimental features and to produce robust quantitation of the surface roughness of human erythrocytes. Air-dried or fixed stained RBCs are very convenient samples for such a kind of studies as they have robust structures holding membrane-bound proteins firmly in place and stabilizing them against damage or compression by the sharp tip of the apparatus.

The major goals of this investigation have been: (i) to show that, under the experimental conditions chosen, the roughness of the plasma membrane of human RBCs is a morphological parameter at the nanometer scale which is independent from the overall cell's shape (i.e., the three-dimensional arrangement of the membrane on the submicron scale can be decoupled from the overall cell's shape); (ii) to reveal the homogeneity of the roughness value when measured in different areas of a single cell and in distinct cells of the same sample, in such a way that the average roughness value can be used as a convenient label to compare different samples; (iii) to explain the usefulness of a surface roughness study by demonstrating the sensitivity of this novel morphological parameter to the RBCs' membrane–skeleton integrity.

2. Materials and methods

2.1. Samples preparation

Blood samples, collected in EDTA as anticoagulant (1.5 mg/ml blood), were obtained from healthy people and, after informed consent, from patients suffering from hereditary spherocytosis (HS) of the Clinic of Haematology, University of Rome "La Sapienza". Samples were immediately diluted 5-fold with buffered isotonic saline containing 5 mM glucose and smears were made by manual spreading. The smears were treated in different ways: (i) kept unfixed and unstained until scanning with the AFM was performed (air-drying method), or (ii) stained by routine May–Grunwald–Giemsa (MGG) technique, or (iii) colored with standard cresyl blue (CB) method, or (iv) treated according to the procedure for scanning electron microscopy until the substitution of the graded ethanol for dehydration with tetramethylsilane (TMS) or hexamethyldisilazane (HMDS). The latter method, in which TMS or HMDS is used (a procedure we will refer to as "SEM drying" independently of the chemical used, since both agents are indistinguishable in their effects on roughness), has been demonstrated equivalent to the critical point drying as far as the preservation of the morphological features of cells is concerned [27–29]. We have preferred these methods for its simplicity and because it does not require metal coating, which would be an unnecessary complication in an AFM study.

When necessary, blood samples (10^9 RBCs/ml) were incubated with 8 or 80 μM (final concentration) cytochalasin D (dissolved in dimethylsulfoxide – DMSO – final concentration 0.2–1% v/v) for 30 min at room temperature before performing smears. These samples were analyzed by AFM, before and after sputtering (see Sputtering and scanning electron microscopy subsection).

When required, RBCs for the scanning electron microscopy analysis of membrane–skeleton were treated according to the protocol described above except that they were deposited on polylysine-treated (10 $mm^2 \times 10$ mm^2 Si (100)) wafers. Afterward, the cells were sputtered by argon ions in order to partially or totally remove the plasma membrane and subsequently coated with 20 nm of gold for the SEM observation.

2.2. The atomic force microscope

The AFM measurements were performed using a home-built microscope described in detail elsewhere [30] and modified to allow also operating in Tapping-mode with a vertical resolution of 1–2 Å. We recall that the instrument, already applied in the study of erythrocytes, [13,15] can be operated under strictly controlled environmental conditions. The AFM measurements were performed at room temperature, in constant 30% relative humidity in both contact and tapping modes.

The contact mode measurements were performed in the weak repulsive regime of constant force with a probe force below 1 nN from zero cantilever deflection. The Tapping mode measurements have been collected in air using Nanodevices (Santa Barbara, CA, USA) Tap150 cantilevers (k=5 N/m, L=125 μm, ν_{res}=150 kHz) operated at constant (typically 10%) damping. The high-resolution images, both in contact and tapping mode, have been collected at a scanning speed of about 3–4 s/row. The reproducibility of data, including the absence of sample damage or alteration due to the measurement procedure, was carefully tested.

2.3. Sputtering and scanning electron microscopy

RBCs were sputtered, according to a recently developed protocol [31], in order to partially or totally remove the plasma membrane without affecting the sub-membrane structures.

The samples to be sputtered were mounted on the ultra high vacuum preparation chamber of the SPHINX X-PEEM microscope [32] in Madison (WI, USA). The base pressure in this chamber was 1×10^{-10} Torr, then, the pressure was raised to a constant value of 1.5×10^{-5} Torr by leaking argon gas into the chamber. Sputtering was performed, using an ion gun (SPECS, model IQE 11/35), placed at approximately 40 cm from the samples, with a constant voltage of 3 kV. Argon sputtering was performed for different times ranging from 5 to 30 min and the samples were, subsequently, coated with a thin layer of Au and characterized by SEM.

The instrument for SEM observation was a Stereoscan 240 (Cambridge Instr, Cambridge, UK) working in high vacuum (below 1×10^{-6} Torr) and operated in a clean room.

2.4. Calculating the RBC's roughness

As it is known, when defining the surface roughness from an AFM image, several parameters of the acquisition method have an influence on the measured value. These parameters include the dependence on the scanned area and, due to the surface statistics (i.e., the fractal or scale-dependent behaviour [33]), on the number of data points. As a consequence, when using the value of roughness for comparison between different samples, the analyzed area must be specified and kept at a constant value as well as the sampling density. The constraints placed on the number of sampling points per image (image size × sampling density) is, however, less critical provided that they are large enough to ensure a solid statistical set (10,000–60,000) with minor difference from image to image. In particular in this paper we used a reference sampling density able to ensure about 20,000 points in 1×1 μm^2 images and 70–80,000 points in 2×2 μm^2 images.

Other factors to be considered are the size and shape of the AFM probe, that is the agent through which the three-dimensional representation of the surface is produced. Indeed, the tip has a finite dimension which, consequently, does not probe the surface profile in an ideal fashion. For instance, it is known that different apical radii and/or different probe forces exerted on the surface during the scan may result in different contact areas (i.e., different resolution). As consequence, the roughness value could be underestimated by an amount that is actually difficult to quantify. In order to evaluate the effect of different contact areas we performed imaging of the very same area of various RBCs (that were very different each other for cells' shape and peculiarities) with different probe forces covering the range we used for the AFM experiments. The subsequent analysis showed negligible variation (around 2%, i.e., well within the experimental errors) of the measured roughness value. Concerning the tip, in our contact mode experiments we used AFM probes with the same expected (statistical) apical radius of 10 mm, height of 3.5 mm and pyramidal shape characterized by an apical angle of 35°. The elastic constant was 0.032 or 0.064 N/m. Unavoidable differences occur in tapping mode which was performed using probes with the same apical radius of the contact probes but slightly different mechanical characteristics (i.e., K=5 N/m, tip height=20 μm, anisotropic apical shape with front angle of 15° and side angle of 17.50°).

The data analysis has been performed using the software package PW-WAVE which allows to both analyze the AFM images and to calculate the roughness value using integrated routines. Concerning the image analysis, no noise filter was applied to the raw data which were treated only by a software background subtraction and, when necessary to have a flat non tilted surface, by a plane alignment and/or by an X axis linearization.

3. Results and discussion

3.1. Preliminary observations on the dependence of the roughness from the AFM parameters

According to the definition of R_{rms} 1.1, the roughness of a RBC's membrane can be associated to the width of the (Gaussian) distribution of the height of the points composing the AFM image of the scanned surface. The height distribution derived from a typical erythrocyte, and the resulting roughness value (measured on a 1×1 μm^2 of surface extent), are given in Fig. 1.

Since the roughness value is expected to depend on the scan size, a measurement of such quantity (in an area range of 0.5 to 2.5 μm^2) on several RBCs belonging to different samples has been determined. Three typical curves are reported in Fig. 2, showing that the increase in roughness as the scan size enlarges follows a very similar trend (in line with previous data on mica, quartz and silicon flat surfaces [5]). In order to make the data treatment simpler and easier, the scrutiny was performed on flat-topped or spherocytic-shaped erythrocytes which are known to physiologically occur even in blood smears from perfectly healthy donors [16].

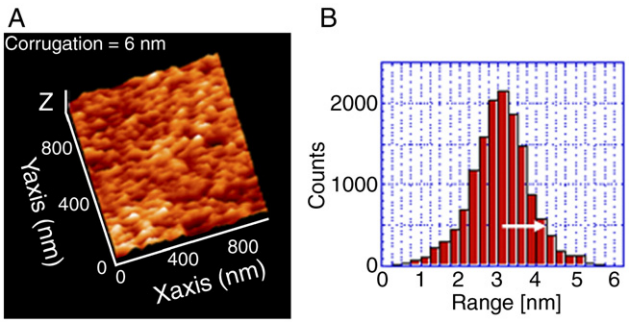

Fig. 1. (A) Three-dimensional topography and (B) distribution of the height (z_i) of all the points composing the AFM topographic image. The R_{rms} value is the width (exemplified by the white arrow) of the distribution shown in panel (B).

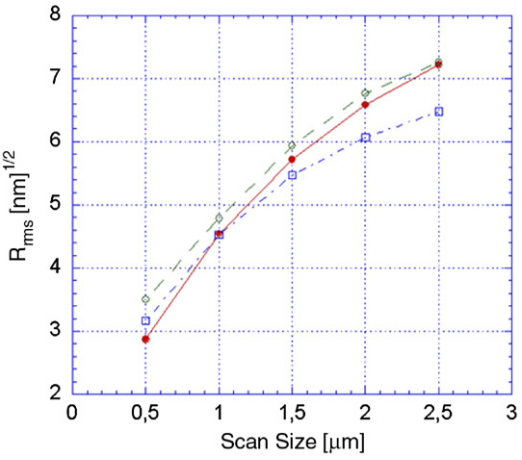

Fig. 2. Examples of the dependence of the roughness value from the size of the (square) sampling field on the RBC's plasma membrane.

The observed trend of roughness vs. scan size, on one hand indicates that the RBC's plasma membrane is a surface-bearing characteristics which allow a proper statistical study and, on the other hand, calls for the choosing of a fixed area to allow an appropriate comparison of the roughness values among different samples. In the following, and except when explicitly differently stated, we will report roughness values measured on areas with the fixed size of 1×1 μm^2.

3.2. Roughness is a sample-related parameter

In a given specimen, the external surface of all RBC is expected to be homogeneous at the scale probed by AFM; accordingly, a good morphological parameter should be bound to values close to one another over the entire cell surface. This expectation has been proved for normal RBCs, as indicated in Figs. 3(A) and (B) where the distribution of roughness values measured in many areas of a single cell follows a sharp Gaussian curve. Therefore, the average roughness value can be considered as a label of the cell.

It is worth stressing that the two Gaussian-like histograms reported in Figs. 1 and 3, although somehow similar in the appearance, are strongly different in the meaning, and in fact, contain distinct information. In particular, the width of the two distributions are associated, respectively, to (Fig. 1) the roughness value of a single sampling and (Fig. 3) to the error bar associated to the measurement of the average roughness of a cell (which, obviously, fits the centre of the Gaussian). In the following, we will make use of histograms of the second kind.

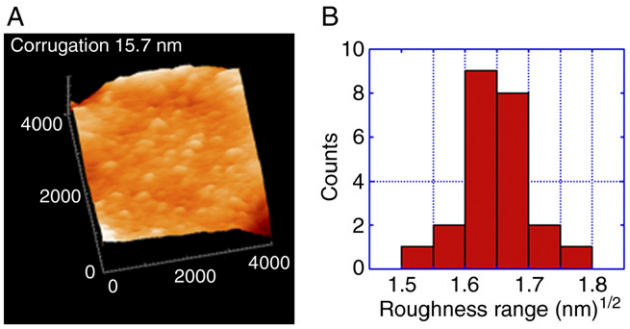

Fig. 3. (A) AFM topography of a RBC. (B) Distribution of the roughness values measured in many different areas above the cell surface. The typically observed sharp distribution of (B) allows to use the average value of all the roughness sampling as a label of the cell.

In order to ascertain whether the roughness value of one cell is representative of a RBC specimen in its entirety, the distribution of the mean roughness values calculated for single cells, and the distribution of the roughness value as a whole have been analyzed. In other words, we sampled the roughness value in different areas of a given cell and repeated the operation in many cells of a fixed specimen. Then, we compared the distribution of the single cells' mean roughness with the distribution of all the roughness values with no regard to the cell where they have been collected. If the single cells in the samples are equivalent, we expect two closely related distribution.

Indeed, comparison of the two distributions, reported in Fig. 4, clearly points to a strongly similar content of information. In particular, the great majority of the cells (mean cell value) and of the single sampling (with no regard to the cell where they have been measured) fall in the neighbourhood of the overall average roughness value with an error (width of the distribution) close to 10% of the mean value. Thus, within this level of confidence, we can assume that the average roughness value (mean of all the performed sampling) can be used as a label of a whole sample.

It is worth noting that in both distribution curves (see Fig. 4) a small number of sampling significantly departs from the mean value. This is an important indication that in almost all specimens there are a small number of erythrocytes which, in terms of membrane roughness, behave differently with respect to the "typical" cell: in particular, our approach is able to make plain and clear the presence of such an RBC class and to estimate its percentage (see also Fig. 5). Moreover, even though, at present, it is not possible to assign these peculiar roughness properties to a special class of RBCs (e.g., very young, very old, unusually shaped cells etc.), it is interesting to observe that this

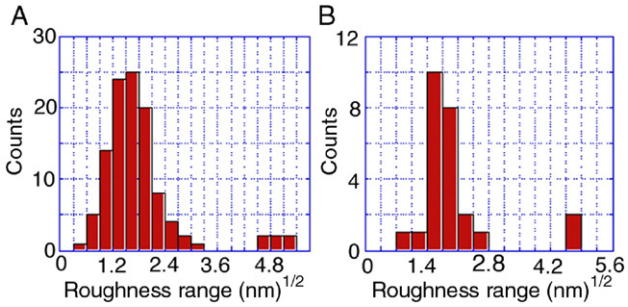

Fig. 4. Comparison between the distribution of all the measured roughness value (panel A) and the distribution of the mean roughness calculated for the single sampled cells (panel B). The two distributions have equivalent results indicating that the whole distribution is coherent with the behaviour of the single cells composing the sample. In both cases, the width of the distribution can be assumed as error associated to the mean value (probability that 66% of the data fall within mean ± width). Typical width values are close to 10% of the mean value of the distribution (slightly smaller for the distribution of the mean cell values).

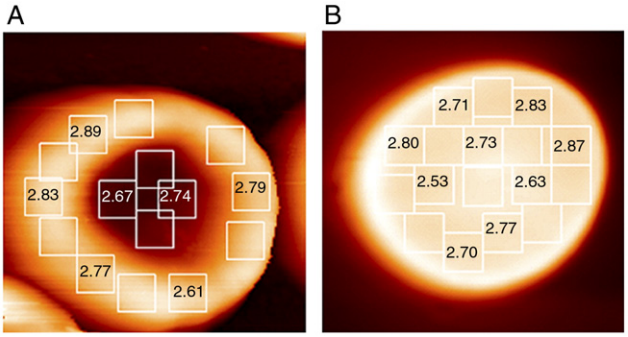

Fig. 5. Panels (A) and (B) (both 8.5 × 8.5 μm) show two differently shaped RBCs from the same healthy donor. Many roughness sampling has been performed on the surface of the cells (in the white squares; some of the values have been explicitly reported). The data show that the roughness is negligibly affected by the different cell's shape.

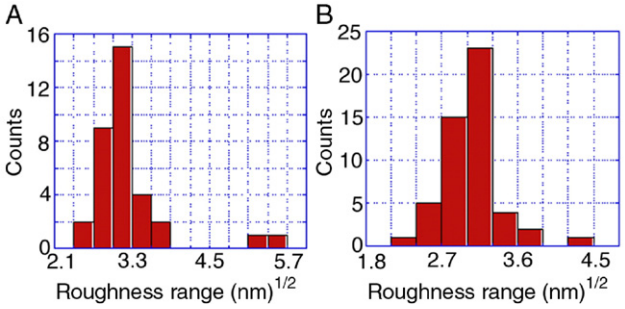

Fig. 6. A statistical demonstration of the independence of the average roughness from the overall cell's shape. Panels (A) and (B) show the histograms of the roughness sampling collected from, respectively, many biconcave and flat-topped cells (including, but not limited to the ones showed in Fig. 5) from the very same sample show a good general agreement and negligible differences in the average roughness value.

percentage can contribute to a quantitative description of the sample's status.

Another important question is whether or not the calculated roughness values are related to the overall RBC's shape (e.g., whether the surface texture is identical or different in normal doughnut-shaped cell and in spheroid or swollen cells present in one sample). As well known, the roughness is a parameter which is best measured on flat surfaces; however, this requirement for flatness might cause some hardship in studying the RBCs roughness, for the normal biconcave cells offer little chance to scan large enough, non-bended surfaces. To evaluate the consequence of this operative difficulty, the mean roughness values measured on cells with sharply different overall shape (spherocyte vs. biconcave disks) occurring in the very same blood smear have been analyzed and compared. For a trustworthy comparison, it is important that the areas chosen on the biconcave RBCs lie as much as possible on a horizontal plane with no residual tilt nor background curvature which would corrupt the analysis.

A direct comparison of two RBCs present in the very same sample, from a healthy donor, which were different in their overall shape, is reported in Fig. 5. No significant divergence in the membrane roughness value can be detected. To further support this observation, a statistical analysis of the mean roughness value measured on a number of flat-topped and of normal biconcave cells from the very same sample has been carried out. The results, reported in Fig. 6, confirmed that the membrane roughness is not affected by the overall cell shape.

This result is not contradictory because, in principle, there is no reason for a straightforward correlation between the overall shape of the cell and the morphology of the membrane measured on the submicron scale. Yet, the finding is a relevant outcome since: (i) it ensures that roughness can be measured with equal confidence on differently shaped cells from the very same sample, and (ii) it demonstrates that, in the blood of an healthy donor, the plasma membrane has the same texture irrespective of the cell overall shape, and the roughness value is a measure of the morphological characteristics at nanometer scale of the RBCs' surface.

As a whole, the above reported consideration can be summarized in the statement that the measurement of the surface roughness of RBCs is a morphological parameter independent from the overall cell shape but characteristic of the single cells composing a given sample. Thus, the average roughness can be used to label a whole sample.

Lastly, in order to learn whether commonly used fixing and/or staining treatments affect the surface roughness of RBCs, the R_{rms} value derived for an air-dried blood smear has been compared with that measured in various smears prepared from the very same blood sample drawn from an healthy donor. In particular, the cells have been (i) stained with cresyl blue, (ii) fixed and colored with May–Grunwald–Giemsa, and (iii) processed as in the case of scanning electron microscopy (see under Materials and methods). The results of the statistical analysis performed in terms of the average value resulting from all the roughness measurements performed on a number of cells belonging to each sample are reported in Table 1 demonstrating that the R_{rms} values (identified as a sample label) can be considered identical – within the experimental error – for all the analyzed specimens. In other words, very different methods of sample handling, which involve exposure of the cells to rather diverse chemicals and/or to various dehydration forces do not affect those structural properties of the erythrocytes that directly influence the roughness values measured by AFM. Another consequence of these data is that a reference roughness value

Table 1
Average roughness value measured on differently prepared normal cells

Sample	R_{rms} $(nm)^{1/2}$	Error $(nm)^{1/2}$	Total no. of sampling
Air dried	3.14	0.43	194
Stained (Cresil Blue)	3.34	0.47	84
Fixed stained (MGG)	3.25	0.44	196
Fixed dehydrated (HMDS drying)	3.30	0.47	96

The distributions of the measured roughness values were found to follow a Gaussian curve (reminiscent of the ones in Figs. 4(A) and (B)), thus, the experimental error associated to the average R_{rms} can be identified with the width of the distribution itself. Simple air drying as well as ordinary treatments used for fixing and/or staining the samples do not affect the measured roughness value. The experiments have been repeated twice.

can be assigned to a given healthy RBC sample without taking into account whether or not it has been fixed and/or stained.

3.3. Surface roughness as a tool for investigating the membrane–skeleton integrity

In order to study this problem in depth, the roughness of normal RBCs has been compared with those of erythrocytes bearing an abnormal membrane–skeleton due to the occurrence of genetic pathologies (hereditary spherocytosis) and with artificially produced flat-topped cells. Hereditary spherocytosis is a highly variable inherited disorder of RBCs determining loss of the network integrity due to genetic mutations in membrane proteins which make up the membrane–skeleton [34]. As a consequence of the membrane–skeletal alteration, the mechanical properties of the spherocytes degrade and the percentage of observable swollen cells into the sample increases dramatically. The artificially swollen cells were obtained by maintaining the cells in slightly (280 mOsm) hypotonic medium which changes the overall RBCs' shape without affecting their membrane–skeleton.

The most impressive result of the statistical analysis reported in Table 2 is the remarkably smaller value of roughness (−50%) observed in pathological samples relative to the native and swollen RBCs, while the roughness remains unchanged when measured on biconcave or swollen cells from normal donor. Considering that such a large reduction in roughness cannot be ascribed to the overall cell shape modification, we hypothesized that the roughness is directly or indirectly sensitive to the membrane–skeleton integrity.

To confirm such an hypothesis, we treated normal cells with cytochalasin, a chemical acting as a cytoskeleton disrupting agent [35] and approached the problems by performing both AFM measurements (which, both on air-dried and on SEM-dried RBCs, were used to calculate the roughness whose value resulted in full agreement with that of RBCs from spherocytosis) and direct visualization of the fibers by SEM. In particular, the SEM visualization was performed on a second aliquot of the very same cells used for the AFM measurement. To achieve this latter purpose, air-dried or SEM-dried RBCs have been sputtered for different times in order to partially or totally remove the lipid bilayer [31], thus enabling a direct observation by SEM of the network filaments constituting the membrane–skeleton. The results are reported in Fig. 7, where the skeleton of both cytochalasin-treated and untreated cells is visualized and compared. Untreated cells show patches of the intact skeleton network, whose architecture remains substantially unaltered while large holes (and sometimes thickening of the filaments) can be observed in samples incubated with both 8 and 80 μM cytochalasin. Therefore, a large decrease in the surface roughness value is indicative of membrane–skeleton alterations produced by destabilization of the filament network.

It is worth noting that the direct observation of the RBC's membrane–skeleton after cytochalasin treatment can be regarded itself as an evidence of the effectiveness on erythrocytes of such a chemical, whose effect is already well known on cell's cytoskeleton.

Table 2
Roughness data for several samples bearing genetic (spherocytes) or artificially induced (cytochalasin treatment) membrane skeleton alterations

Sample	R_{rms} $(nm)^{1/2}$	Error $(nm)^{1/2}$	Total no. of sampling
Spherocytes (1)	1.69	0.35	170
Spherocytes (2)	1.47	0.22	98
Artificially swollen	3.11	0.40	204
Air dried	3.14	0.43	194
Air dried+DMSO	3.10	0.44	95
Air dried+cytochalasin (80 μM)	1.56	0.17	218
HMDS drying+cytochalasin (8 μM)	1.81	0.39	104
HMDS drying+cytochalasin (80 μM)	1.70	0.50	114

The two samples of spherocytes are from patients with different clinical spectra (more severe for no. 2). A control as well as a sample composed of normal cells artificially swollen by maintenance in (280 mOsm) hypotonic medium, in which the cells have the same shape of spherocytes but no skeletal alteration, were considered for comparison. The roughness of normal cells treated with DMSO which was used to vehiculate cytochalasin into the RBCs was also reported. Low roughness was detected after cytochalasin treatment both on air-dried and on fixed–post fixed-dehydrated RBCs (HMDS—*also called SEM-dried*). For further comparisons, the average roughness calculated on the subclass of flat-topped cells occurring in air-dried (3.09), stained (3.26), fixed-stained (3.34) and in fixed–post fixed and dehydrated cells (3.24) showed high roughness values.

3.4. Dependence of the Roughness value on the AFM mode of operation

As a last topic, we tried to ascertain the possible dependence of the measured roughness value on the AFM mode of operation: namely, contact mode or tapping mode.

As is well known, AFM images are three-dimensional representations of surfaces obtained through the monitoring of continuous or intermittent loading forces of a sharp tip on the sample surface. The major physical difference between contact and tapping modes of operation rests on the intensity of the forces applied on the sample's surface during the scan and, therefore, on the magnitude of the small but unavoidable deformation of the sample. In particular, in tapping mode the vibrating tip barely taps the sample's surface at the bottom of its oscillation thus leading to a drastic reduction (up to two order of magnitude in comparison to contact mode) of the lateral forces between tip and specimen. The physical differences between these two AFM modes could have some effect on the quantitative observation of the surface texture. Therefore, three air-dried specimens (native RBCs, cytochalasin-treated RBCs, and hereditary spherocytes) have been analyzed in both contact and tapping mode and, for sake of the comparison, all results are reported in Table 3. It is evident that the average roughness values measured in tapping mode are smaller with respect to contact mode; and yet, regardless on the AFM mode of operation, the roughness measured on normal cells is much higher than on cells whose membrane–skeleton integrity is compromised (either genetically or by cytochalasin). This is, indeed, expected for a morphological parameter linked to some intrinsic difference between different classes of cells such as, in our case, their membrane–skeleton structure.

Since in most studies performed on soft samples the tapping mode leads to higher resolution images, it could be surprising

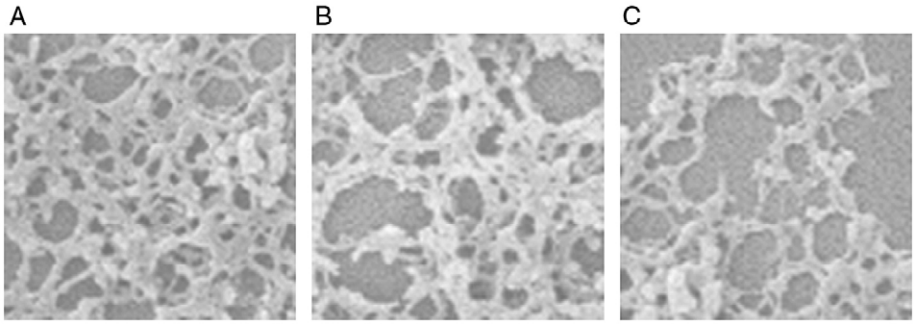

Fig. 7. Panel (A—500 nm) shows a normal RBCs sputtered for 20 min. An almost intact membrane–skeletal network can be observed. Panels (B and C—500 nm) show, respectively erythrocytes treated with 8 μM and 80 μM cytochalasin observed after 20 min of sputtering. A progressive, cytochalasin-dependent, destruction of the membrane–skeleton is evident.

that lower texture values have been obtained. This apparent inconsistency finds a simple explanation in the following consideration based on how an AFM works. In a simple model, the loss of water during drying promotes a micro-sinking inwards of the lipid bilayer at the places where there is a lesser support by the membrane–skeleton, leaving behind the protein filaments forming the skeleton network [23,35]. During scanning in contact mode, the AFM tip extends the depressions of the spontaneous sinking by exerting higher forces on the cell surface than that produced in tapping mode. Therefore, an existing difference in the mean roughness value can be magnified by the AFM mode of operation: in particular elastic membrane micro-deformations determined in contact mode by the larger scanning forces enhance the detection of the existing differences in the cell skeleton. As a consequence, the scanning in contact mode can be preferable for the investigation of the modifications of the membrane–skeleton in intact RBCs.

Taking into account the mechanical characteristics of the plasma membrane (including deformability, different support of intact membrane–skeleton compared to corrupted networks [36] and tip compliance), the occurrence of high roughness values on normal cells and of low values on skeleton defective RBCs can be explained by the same model. In particular, a mechanism of (elastic) flattening of the surface structures at the nanoscale during the contact with the probe can occur, and is expected to be larger for unsupported membranes then for normal cells, thus resulting in higher or lower measured roughness value.

Table 3
Roughness value measured using different mode of operation of the AFM

Sample	Mean roughness from contact mode images	Mean roughness from tapping mode images
Freshly prepared air dried	3.10±0.32	2.60±0.31
Freshly prepared+ cytochalasin	1.64±0.23	1.40±0.20
Hereditary spherocytosis	1.43±0.20	1.35±0.22

The reported value for normal, spherocytes and (80 μM) cytochalasin treated erythrocytes, is the average value of all the roughness measurements performed on a number of cells (typically 40) from each samples. The reported error is the standard deviation. The experiments have been repeated twice with the same resulting trend. The roughness value of the control sample measured in contact mode agrees with what measured in the previously performed experiments of Table 1.

In the present paper, it has been demonstrated that the surface texture at nanometer scale of air-dried RBCs can be conveniently described by a single numerical value: the average surface roughness. Such a parameter, very useful to compare the characteristics of surfaces, has been hardly used, up to now, to study cell's membrane, and yet it has been found to be a surprisingly powerful tool in our approach. Clearly, to overcome the complications introduced by the intrinsic variability of biological samples in terms of structural parameters, a certain degree of standardization in the procedure of AFM data collection and analysis is necessary. Furthermore, to increase the reliability of the presented data, all the results of this study are supported by a robust statistical analysis which involved a large number (typically 100–200) of sampling of the desired parameters. In this endeavour the simplicity of our mathematical approach, based on the R_{rms} roughness definition (Eq. (1.1)), is a critical advantage. With this premise, the membrane roughness, independent from the various overall shapes of the RBCs, represents a basic characteristic of the cells composing a specimen and thus, as a remarkable practical consequence, can be used as a label of the whole sample. A deeper discussion on this subject could be useful: the surface roughness is a morphology-related parameter which can be compared to another morphological parameter such as the overall cell shape. There is no reason to assume "a priori" that an overall change of the cell's shape must be linked to the arrangement, on a totally different length scale, of its plasma membrane, thus, if there is a correlation between these parameters it must be demonstrated. In this framework we provided evidences that, in all the analyzed cases, there is no correlation between the overall shape of a cell and the arrangement of its plasma membrane evaluated, with a spatial resolution about three orders of magnitude smaller then the RBC size, through its roughness value.

Furthermore, this study has also indicated the average roughness value of a sample to be the same for RBCs (coming from one source) under many non-physiological conditions associated to a variety of treatments commonly used for fixation and/or staining and/or drying the cells. Such methods are currently used in clinical and forensic medicine to prepare and analyze blood smears.

In terms of applications, we have presented an approach to the study of erythrocytes integrity through a method based on

the analysis of their surface roughness. The study, which required the definition of a base protocol for a proper roughness-based comparison between different samples, demonstrated that the mean roughness value is very sensitive to cytoskeletal alterations both of pathological and artificial origin. The mechanism which allows detection of the status of underlying cell structure by analyzing, in a simple and non-destructive way, the morphology of the overlying plasma membrane, has been suggested to be a consequence of the different mechanical characteristics (elasticity, compliance etc.) of properly supported or unsupported membranes. Such intrinsic features can be enhanced or reduced by the AFM imaging parameters (i.e., by working in contact or tapping mode) resulting in larger of smaller differences between intact and membrane–skeleton-defective cells.

In conclusion, the use of roughness in evaluating biological surfaces provides a non-destructive, simple and powerful tool for a novel approach with the potential to label whole samples and yet to detect the single-cell status through an ultrastructural morphological analysis. In this context, AFM has been proven a useful tool for quantitative biophysical studies such as, for instance, comparing (i) changes in the surface texture of RBCs coming from a single donor (e.g., as a function of some disease or, more intriguing, in the physiological process of cell aging), or (ii) ultrastructural differences between RBCs' samples originating from diverse sources.

As future work, deeper insights into the relationship between roughness values and surface structure could be gained by considering the overall shape of the height distribution deduced from the AFM image, which can be Gaussian or not, and, possibly, by taking into account the higher order momenta of the distribution.

Acknowledgments

The authors are grateful to Prof. Susanna Feru together with the clinical staff of the Department of Cellular Biotechnology and Haematology, University of Rome 'La Sapienza', for their support and blood samples. We also wish to thank Dr. Giovanni Longo for the help he provided during some AFM measurements and for the helpful discussion.

References

[1] D. Bonnell, Scanning Probe Microscopy and Spectroscopy: Theory, Techniques and Applications, John Wiley & Sons, New York, 2000.
[2] V.J. Morris, A.R. Kirby, A.P. Gunning, Atomic Force Microscopy for Biologists, Imperial College Press, 1999.
[3] N.R. Washburn, K.M. Yamada, C.G. Simon Jr., S.B. Kennedy, E.J. Amis, High-throughput investigation of osteoblast response to polymer crystallinity: influence of nanometer-scale roughness on proliferation, Biomaterials 25 (2004) 1215–1524.
[4] J. Katainen, M. Paajanen, E. Ahtola, V. Pore, J. Lahtinen, Adhesion as an interplay between particle size and surface roughness, J. Colloid Interface Sci. Sep. 14 (2006) (Electronic publication ahead of print).
[5] G.J. Simpson, D.L. Sedin, K.L. Rowlen, Surface roughness by contact versus tapping mode AFM, Langmuir 15 (1999) 1429–1434.
[6] C. Yang, U. Tartaglino, B.N. Persson, Influence of surface roughness on super-hydrophobicity, Phys. Rev. Lett. 97 (2006) 116103–116106.
[7] M. Lombardo, M.P. De Santo, G. Lombardo, R. Barberi, S. Serrao, Analysis of intraocular lens surface properties with atomic force microscopy, J. Cataract Refract. Surg. 32 (2006) 1378–1384.
[8] C.V. Ramana, S. Utsunomiya, R.C. Ewing, C.M. Julien, U. Becker, Structural stability and phase transitions in WO3 thin films, J. Phys. Chem., B 110 (2006) 10430–10435.
[9] B.S. Bull, Morphology of the erythron, in: E. Beutler, M.A. Lichtman, B.S. Coller, T.J. Kipps, U. Seligsohn (Eds.), Williams Hematology, 6th ed., McGraw-Hill, New York, 2001, pp. 271–288.
[10] A. Elgsaeter, A. Mikkelsen, Shapes and shape changes in vitro in normal red blood cells, Biochim. Biophys. Acta 1071 (1991) 273–290.
[11] M.P. Sheetz, S.J. Singer, Biological membranes as bilayer couples. A molecular mechanism of drug–erythrocyte interactions, Proc. Natl. Acad. Sci. U. S. A. 71 (1974) 4457–4461.
[12] J.E. Ferrell, K.-J. Lee, W.H. Huestis, Membrane bilayer balance and erythrocyte shape: a quantitative assessment, Biochemistry 24 (1985) 2849–2857.
[13] M. Girasole, A. Cricenti, R. Generosi, A. Congiu Castellano, F. Boffi, A. Arcovito, G. Boumis, G. Amiconi, Atomic force microscopy study of erythrocyte shape and membrane structure after treatment with a dihydropyridinic drug, Appl. Phys. Lett. 76 (2000) 3650–3652.
[14] N. Mohandas, J.A. Chasis, Red blood cell deformability, membrane material properties and shape: regulation by transmembrane, skeletal and cytosolic proteins and lipids, Semin. Hematol. 30 (1993) 171–192.
[15] M. Girasole, A. Cricenti, R. Generosi, A. Congiu-Castellano, G. Boumis, G. Amiconi, Artificially-induced unusual shapes in erythrocytes: an atomic force microscopy study, J. Microsc. 203 (2001) 1–8.
[16] L.O. Simpson, Blood from healthy animals and humans contain nondiscocytic erythrocytes, Br. J. Hematol. 73 (1989) 561–564.
[17] Z. Shao, J. Mou, D.M. Czajkowsky, J. Yang, J.Y. Yuan, Biological atomic force microscopy: what is achieved and what is needed, Adv. Phys. 45 (1996) 1–86.
[18] P. Zachée, M. Boogaerts, J. Snauwaert, L. Hellemans, Imaging uremic red blood cells with the atomic force microscope, Am. J. Nephrol. 14 (1994) 197–200.
[19] W. Han, J. Mou, J. Sheng, J. Yang, Z. Shao, Cryo atomic force microscopy; a new approach for biological imaging at high resolution, Biochemistry 34 (1995) 8215–8220.
[20] P. Zachée, J. Snauwaert, P. Vandenberghe, L. Hellemans, M. Boogaerts, Imaging red blood cells with the atomic force microscope, Br. J. Hematol. 95 (1996) 472–481.
[21] H.J. Butt, E.K. Wolff, S.A.C. Gould, B. Dixon Northern, C.M. Peterson, P.K. Hansma, Imaging cells with atomic force microscope, J. Struct. Biol. 105 (1990) 54–61.
[22] L. Di, W. Liu, Y. Liu, J.Y. Wang, Effect of asymmetric distribution of phospholipids in ghost membrane from rat blood on peroxidation induced by ferrous ion, FEBS Lett. 580 (2006) 685–690.
[23] M. Takeuchi, H. Miyamoto, Y. Sako, H. Komizu, A. Kusumi, Structure of the erythrocyte membrane skeleton as observed by atomic force microscopy, Biophys. J. 74 (1998) 2171–2183.
[24] A.H. Swihart, J.M. Mikrut, J.B. Ketterson, R.C. MacDonald, Atomic force microscopy of the erythrocyte membrane skeleton, J. Microsc. 204 (2001) 212–225.
[25] R. Lal, B. Drake, D. Blumberg, D.R. Saner, P.K. Hansma, S.C. Feinstein, Imaging real-time neurite outgrowth cytoskeletal reorganization with an atomic force microscope, Am. J. Physiol. 269 (1995) C275–C285.
[26] J.K. Horber, J. Mosbacher, W. Haberle, J.P. Ruppersberg, B. Sakmann, A look at membrane patches with a scanning force microscope, Biophys. J. 68 (1995) 1687–1693.
[27] S. Dey, A new rapid air-drying technique for scanning electron microscopy using tetramethylsilane: application to mammalian tissue, Cytobios 73 (1993) 17–23.
[28] D.F. Bray, J. Bagu, P. Koegler, Comparison of HMDS and critical point drying methods for scanning electron microscopy of biological specimens, Microsc. Res. Tech. 26 (1993) 489–495.
[29] F. Braet, R. De Zanger, E. Wisse, Drying cells for SEM, AFM and TEM by hexamethyldisilazane: a study on hepatic endothelial cells, J. Microsc. 186 (1997) 84–87.

[30] A. Cricenti, R. Generosi, Air operating atomic force-scanning tunnelling microscope suitable to study semiconductors, metals and biological samples, Rev. Sci. Instrum. 66 (1995) 2843–2847.
[31] G. De Stasio, B.H. Frazer, M. Girasole, L.M. Wiese, E.K. Krasnowska, G. Greco, A.L. Serafino, T. Parasassi, Imaging the cell surface: argon sputtering to expose inner cell structures, Microsc. Res. Tech. 63 (2004) 115–121.
[32] B.H. Frazer, M. Girasole, L.M. Wiese, T. Franz, G. De Stasio, Spectromicroscope for the photoelectron imaging of nanostructures with X-rays (SPHINX): performance in biology, medicine and geology, Ultramicroscopy 99 (2004) 87–94.
[33] J. Krim, I. Heyvaert, C. van Haesedonck, Y. Bruynseraede, Scanning tunnelling microscopy observation of self-affine fractal roughness in ion-bombarded film surfaces, Phys. Rev. Lett. 70 (1993) 57–60.
[34] S.C. Liu, L.H. Derick, P. Agre, J. Palek, Alteration of the erythrocyte membrane skeletal ultrastructure in hereditary spherocytosis, hereditary elliptocytosis and pyropoikilocytosis, Blood 76 (1990) 198–205.
[35] E. Henderson, P.G. Haydon, D.S. Sakaguchi, Actin filament dynamics in living glial cells imaged by atomic force microscopy, Science 257 (1992) 1944–1946.
[36] J. Sleep, D. Wilson, R. Simmons, W. Gratzer, Elasticity of the red cell membrane and its relation to hemolytic disorders: an optical tweezers study, Biophys. J. 77 (1999) 3085–3095.